Conservative and dissipative force imaging of switchable rotaxanes with frequency-modulation atomic force microscopy

Alan A. Farrell,[1,*] Takeshi Fukuma,[2] Takayuki Uchihashi,[1] Euan R. Kay,[3] Giovanni Bottari,[3] David A. Leigh,[3,†] Hirofumi Yamada,[2] and Suzanne P. Jarvis[1]

[1]*Nanoscale Function Group, Centre for Research on Adaptive Nanostructures and Nanodevices, University of Dublin, Trinity College, Dublin 2, Ireland*

[2]*Department of Electronic Science and Engineering, Kyoto University A1-326, Katsura, Nishikyo, Kyoto 615-8510, Japan*

[3]*School of Chemistry, University of Edinburgh, The King's Buildings, West Mains Road, Edinburgh EH9 3JJ, UK*

(Received 27 May 2005; published 23 September 2005)

We compare constant amplitude frequency modulation atomic force microscopy (FM-AFM) in ambient conditions to ultrahigh vacuum (UHV) experiments by analysis of thin films of rotaxane molecules. Working in ambient conditions is important for the development of real-world molecular devices. We show that the FM-AFM technique allows quantitative measurement of conservative and dissipative forces without instabilities caused by any native water layer. Molecular resolution is achieved despite the low Q-factor in the air. Furthermore, contrast in the energy dissipation is observed even at the molecular level. This should allow investigations into stimuli-induced sub-molecular motion of organic films.

DOI: 10.1103/PhysRevB.72.125430 PACS number(s): 68.37.Ps, 81.16.Fg, 81.07.Nb, 68.43.Fg

I. INTRODUCTION

In Frequency Modulation Atomic Force Microscopy (FM-AFM) a cantilever with a nanometer-sized probe is self-oscillated at its resonant frequency. Small changes in the resonance can be readily detected corresponding to a force interaction between tip and sample. In an ultrahigh vacuum (UHV) environment the technique is capable of imaging surfaces with true atomic resolution regardless of conductivity.[1–3] This is important for organic material applications, since most organic materials have poor conductivity. Indeed, molecularly resolved images of organic adsorbates in UHV have been presented.[4–7] In addition the entire distance range of the force interaction can be unambiguously quantified without instabilities.[1,8–10] The FM-AFM technique can also distinguish between conservative and dissipative forces, see, for example, Ref. 11. The conservative tip-sample force interaction results in a reversible change with distance in the cantilever resonance, without any loss of cantilever vibrational energy. On the other hand, the dissipative force interaction results in the loss of the cantilever vibrational energy. In the constant amplitude FM-AFM mode a feedback loop keeps the oscillation amplitude constant. The energy dissipation caused by the tip-sample interaction in FM-AFM is manifested as an increase in the excitation amplitude. This dissipation can be quite large, anywhere from 0.1 to a few eV depending on the sample, the interaction area, and the environment,[12,13] and moreover can be imaged at a single molecular or even atomic scale.[12,14] In the context of molecular thin films, dissipation is thought to be related to the local mechanical properties of the sample.

Real world chemical and biological applications require operation in air or liquid environments. In the liquid environment, where meniscus forces are not present, the FM-AFM technique is being adopted.[15–19] In ambient conditions the presence of any native water layer limits the imaging resolution and resolution of the full range of the force interaction. Some FM-AFM experiments in air have also been presented.[20] Recently Sasahara *et al.* imaged oxygen-atom vacancies as depressions in oxygen atom rows in a controlled dry N_2 environment after back-filling of a UHV chamber.[21] Fukuma *et al.* also imaged a hydrophobic alkanethiol SAM with true-molecular resolution.[22] Hölscher *et al.* used the constant excitation FM-AFM method to quantify the force in ambient conditions valid for large cantilever oscillation amplitudes.[23,24] Using the related dynamic technique of amplitude modulation AFM (AM-AFM) with ~1 nm cantilever oscillation amplitudes in the attractive force regime, Anselmetti *et al.* reported single molecular resolution of a hexagonal packed intermediate protein layer.[25] By monitoring the Q-factor of the cantilever as a function of tip-sample distance an indication of the energy dissipation was provided. For realistic future applications including molecular sensors the constant amplitude FM-AFM technique should be important for molecular-scale investigations; the advantages of the technique make it useful for the imaging of soft and easily damaged samples without the high loading forces associated with contact mode AFM, while offering high spatial resolution and the possibility for single molecule sensing, and with the capability of distinguishing the conservative and dissipative force interaction. In this study we consider an FM-AFM experiment carried out in UHV and show comparable results in air. We discuss the important information that can be obtained with the technique in relation to a specific system of rotaxane molecules. This information includes qualitative imaging, high-resolution imaging, exact determination of the force irrespective of the oscillation amplitude, and quantitative energy dissipation imaging at different length scales.

Rotaxanes are molecules with two parts—the "thread" (a chain-like section with two bulky stoppers) and the macrocycle—that are mechanically interlocked but not covalently linked. The macrocycle is situated most of the time at stable low energy sites on the thread, where optimal noncovalent inter-component interactions are achieved. Relative

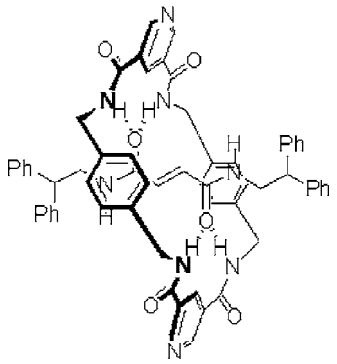

FIG. 1. Molecular structure of exopyridyl fumaramide rotaxane (EFR).

motion of the two components is driven by Brownian motion and can be controlled by altering the binding affinity between the macrocycle and different parts of the thread.[26] Since organic molecules show characteristic electrical and/or optical properties that are greatly sensitive to the molecular structure and conformation, rotaxane molecules have attracted a lot of attention as possible future molecular devices.[27–29] The molecules in this study are constructed from a fumaramide-containing thread, around which a benzylic amide macrocycle is assembled in a hydrogen-bond directed process.[30] In solution, the macrocycles exhibit continuous rotational ("pirouetting") motion with respect to the thread. Upon irradiation at 254 nm, the fumaramide (*trans*-double bond) unit is switched to a maleamide (*cis*-double bond) unit and in solution it is found that this results in an increase in the rate of macrocyle pirouetting by a factor of 10^6.[31] Other similar benzylic amide rotaxanes can have different kinds of switching behavior,[32–34] and from the results of the simple molecule used in this paper we may predict some of their behavior on a surface. In the solid-state such molecules are usually immobilized in a fixed conformation due to intermolecular hydrogen bonding.[35] The extra degrees of freedom associated with surface immobilization however, have been shown to permit sub-molecular motions and switching processes in a number of interlocked architectures.[36–45] Light switching of the properties of other types of organic thin films has also been demonstrated.[46–50] Using single-molecule force spectroscopy, where a long polymer chain was stretched between tip and sample, light-induced switching of an azobenzene polymer was directly observed on a molecular scale.[51] If we can develop dissipation imaging in ambient conditions on this model rotaxane system this technique may provide the opportunity to study externally stimulated sub-molecular motion at the local molecular level simultaneously with topography in this practical environment.

II. EXPERIMENT

The synthesis of fumaramide rotaxane molecules has been described elsewhere and the exopyridyl version used in this study (as shown in Fig. 1) was prepared by an analogous method.[30] Samples were prepared by dropping from acetone solution (HPLC grade, Aldrich). 0.005 mM solutions of exopyridyl fumaramide rotaxane were dropped (14 μl/cm^2) onto a freshly cleaved HOPG surface (ZYA quality, NT-MDT) to give approximately one monolayer surface coverage. To achieve homogeneous evaporation of the solvent the evaporation speed was reduced by reducing the temperature of the dropped solvent to approximately five degrees by refrigeration. Furthermore, during evaporation the sample was in a closed 500 cm^3 container in the presence of desiccant to prohibit condensation of water on the cold acetone.

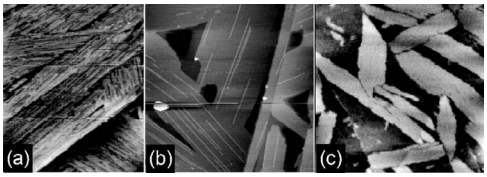

FIG. 2. Meso-scale FM-AFM images of an EFR thin film on HOPG (a) in UHV before annealing (464 nm $\times$ 558 nm, cantilever: Nanosensors NCH, $\Delta f=-15$ Hz, $a=8$ nm), (b) in UHV after annealing (500 nm $\times$ 500 nm, cantilever: NCH, $\Delta f=-20$ Hz, $a=8$ nm), (c) in ambient conditions no annealing (500 nm $\times$ 500 nm, cantilever: Nanosensors EFM, $\Delta f=-25$ Hz, $a=9.6$ nm, $Q=154$).

A commercially available FM-AFM (JEOL JSPM-4500) with some modifications was used for UHV imaging (base pressure: About 1×10^{-7} Pa). The original frequency shift detector was replaced with a newly developed frequency modulation detector.[52] A highly doped *n*-Si cantilever (Nanosensors: NCH) with a resonance frequency of about 300 kHz and a nominal spring constant of 40 N/m was used for FM-AFM imaging. The Q factor measured under UHV conditions was about 30 000. After preparation the sample was immediately placed into the UHV chamber. For annealing, the sample was removed and annealed in air at 150 °C for two hours and re-introduced to the UHV chamber.

An Asylum MFP-3D with some modifications was used for imaging in ambient conditions, operated in FM-AFM mode with piezo activation or magnetically activated cantilevers (MAD-Mode).[53] In the latter method the lever is oscillated by the magnetic field of a current-carrying coil. Using the same Nanosensors NCH cantilevers as above a magnetic particle of NdFeB (with dimensions around 20 microns) was attached with epoxy to the end of the backside of the cantilever. After attachment the resonance of the lever was typically reduced to about 50 kHz. The Q-factor in ambient conditions was around 500. A home-built piezo tube scanner was used for high resolution imaging.

All measurements were performed in the constant frequency shift mode, where the negative frequency shift of the cantilever resonance frequency (Δf) induced by the tip-sample interaction was kept constant during FM-AFM imaging. The cantilever is vibrated at constant amplitude, where the vibration amplitude of the cantilever (a) was kept constant by adjusting the amplitude of a cantilever excitation signal A_{exc}. In this excitation mode, energy dissipation caused by the tip-sample interaction can be estimated from the additional increase of A_{exc}.[54] Thus, the dissipation image was obtained as a two-dimensional map of A_{exc}.

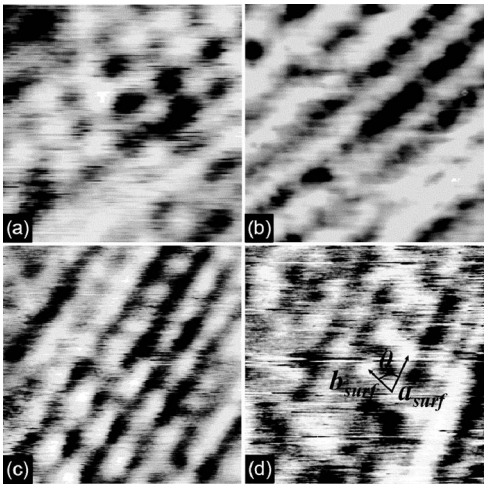

FIG. 3. Molecular-scale UHV FM-AFM images of an EFR thin film on HOPG. (a)–(c) Before annealing and (d) annealed sample, {(a): 9 nm×9 nm, $\Delta f=-150$ Hz, $a=6.5$ nm, (b): 9 nm×9 nm, $\Delta f=-150$ Hz, $a=6.5$ nm, (c): 9 nm×9 nm, $\Delta f=-170$ Hz, $a=6.5$ nm, (d): 9 nm×9 nm, $\Delta f=-180$ Hz, $a=5.9$ nm; measured lattice parameters: $a_{surf}=1.65$ nm±0.1 nm, $b_{surf}=1.35\pm0.1$ nm, $\theta=70°\pm2°$}.

III. RESULTS AND DISCUSSION

Figure 2(a) shows an FM-AFM image of a thin film of expyridyl fumaramide rotaxane on HOPG. The orientation of the domains according to the lattice direction of the substrate shows that the molecule grows epitaxially on graphite. After annealing [Fig. 2(b)] it can be seen that the domain edges are straight and that domains are more clearly defined. The increased uniformity of the surface indicates that the energy provided by the annealing process has resulted in rearrangement of the molecules in a lower energy configuration. Figure 2(c) demonstrates that the shape of the domains can also be evaluated by FM-AFM imaging in air.

Molecular-scale topographic images of the un-annealed sample are shown in Figs. 3(a)–3(c). Individual molecules in the rows can often be resolved, however, no periodic intermolecular distance is found along the rows (stripes in the image) and the rows are also unevenly spaced. The molecules are in a somewhat disordered nonequilibrium arrangement. In the case of the annealed sample [Fig. 3(d)], there is strong periodicity in both directions. This increase in long and short-range order is typical of the annealing process. Heating the sample gives the molecules the extra energy required to move from their local energy minimum and break up the nonequilibrium packing structure. In fact, the measured dimensions of $a_{surf}=1.65\pm0.1$ nm and $b_{surf}=1.35\pm0.1$ nm with $\theta=70°$ strongly suggests a commensurate molecular reconstruction of the form: $\left[\begin{smallmatrix}a_{surf}\\ b_{surf}\end{smallmatrix}\right]=M\left[\begin{smallmatrix}a\\ b\end{smallmatrix}\right]$, where $M=\left[\begin{smallmatrix}7 & 0\\ -1 & 6\end{smallmatrix}\right]$ as illustrated in Fig. 4.

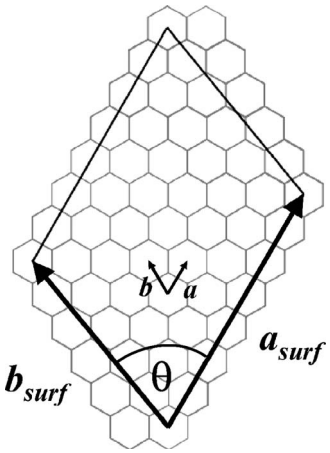

FIG. 4. Apparent equilibrium reconstruction of the EFR film on HOPG after annealing with parameters: $a_{surf}=1.65$ nm, $b_{surf}=1.37$, $\theta=68°$.

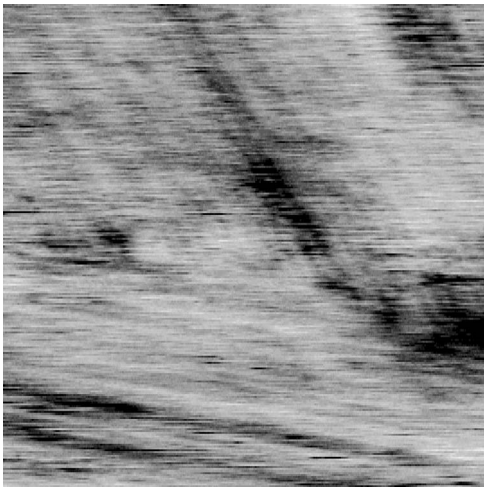

FIG. 5. Molecular-scale ambient FM-AFM topography image of EFR thin film on HOPG (70 nm×70 nm, cantilever: Nanosensors NCHR+magnet, $a=10.8$ nm, $\Delta f=-35$ Hz).

Strong intermolecular interactions in a closely packed film are restrictive to sub-molecular motion so it is not necessarily a good thing that the film is well ordered and it is useful that we are able to access the many nonequilibrium film-structures shown in Figs. 3(a)–3(c).

Figure 5 is a large image taken in ambient conditions, which shows clear molecular-scale features and has been chosen because it shows two neighboring domains and, therefore, true structure, as opposed to periodic noise. The

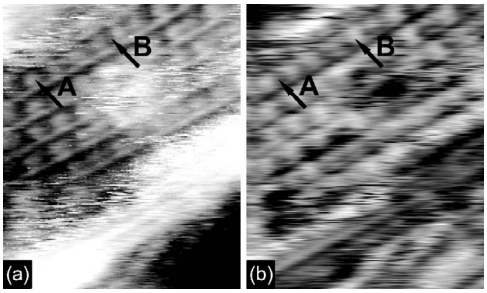

FIG. 6. Molecular-scale UHV FM-AFM images of an EFR thin film on HOPG. Simultaneous topography (a) and dissipation (b) images (23.2 nm×27.9 nm, cantilever: NCH, $\Delta f=-100$ Hz, $a=8.9$ nm).

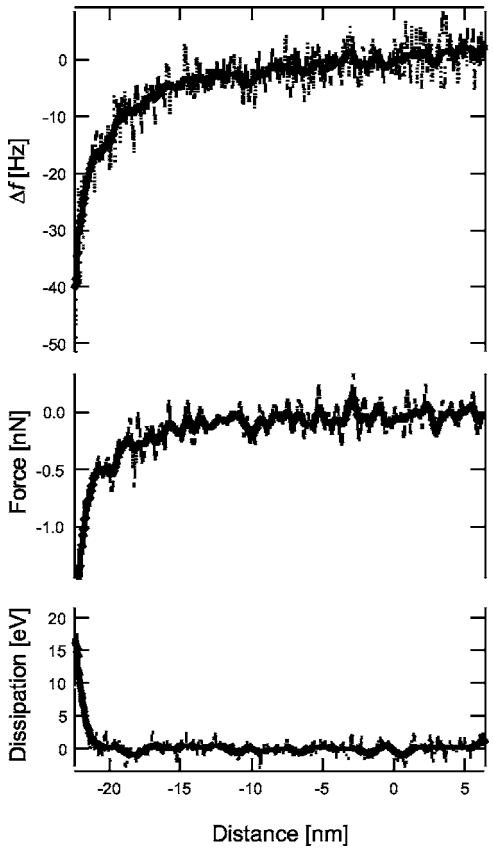

FIG. 7. Typical frequency, force and dissipation vs tip-sample distance curves in ambient conditions, dots: Raw data, line: Smoothed data (Cantilever: NCHR+magnet, $Q=510$, $a=8.9$ nm).

film structure dimensions are consistent with those measured in UHV for the un-annealed sample. Despite the lower Q-factor of the cantilever in air (500) compared to vacuum ($\sim$30 000), the presence of a liquid layer and contamination from long-chain hydrocarbons always present in ambient conditions, the resolution is still very high. The tip can move through the liquid layer while imaging the film, and any surface contamination must only be loosely bound and does not affect the imaging. The FM-AFM technique should thus be useful for the many kinds of study where high resolution is desirable.

The disordered or loose packing commonly found in organic thin films (and hence their stability against the tip-sample interaction force) has a strong influence on the contrast formation in energy dissipation images. Dissipation is increased on less ordered, less well-packed surfaces, both at the molecular scale and the meso scale.[55,56] Fukuma *et al.* showed that the contrasts are probably related to the number of molecules interacting with the tip—the more molecules interacting with the tip the greater the energy transfer; thus at the molecular scale the dissipation image shows inverted contrast relative to the topographic image.[7] Figure 6 shows a molecular-scale topographic image [Fig. 6(a)] of a nonequilibrium arrangement of the rotaxanes and the corresponding map of A_{exc} (dissipation image) [Fig. 6(b)], taken in UHV conditions. The dissipation image displays essentially inverted contrast with respect to the corresponding topographic

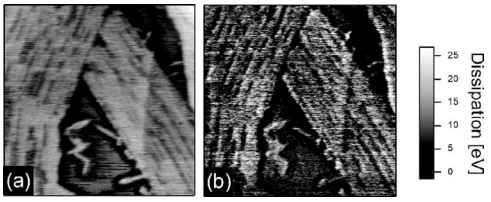

FIG. 8. Meso-scale ambient FM-AFM simultaneous topography (a) and dissipation (b) images of an EFR thin film on HOPG (500 nm$\times$500 nm, $\Delta f=-26$ Hz, $a=11.8$ nm).

image. Arrows A and B mark the same points on each image. Position A corresponds to a tip position directly above a molecule. The internal motion of the molecule provides a coupling pathway and energy is dissipated into the sample. At position B the tip is over an intermolecular space and more than one molecule is involved in the dissipation process and thus the relative contrast is increased in these places. This explains the contrast inversion between the two image types. Images of A_{exc} such as these are easily converted to quantitative images of the average dissipated energy per oscillation.[54]

In ambient conditions the native layer of water adsorbates is often a problem for AFM techniques. "Contact mode," while allowing exact determination of the force, suffers from "jump-to-contact" instabilities (caused when the force gradient is higher than the cantilever stiffness) and adhesion instabilities (caused by a water meniscus between the tip and the local sample area). "Intermittent-contact mode" can overcome these obstacles with large amplitudes and stiffer cantilevers, however, unambiguous determination of the force is difficult with this technique.[57] The FM method with a constant amplitude has the same advantages but allows recovery of the force, which has been demonstrated in liquid and UHV environments.[58,59] Furthermore, in the FM method the attractive and repulsive force regions are easily distinguished which allows for exact control of the force. A portion of the attractive part of the force versus distance curve for a tip with a magnetically activated cantilever in ambient conditions is shown in Fig. 7. Force is calculated from the frequency shift using the method of Sader and Jarvis via the equation:

$$F(z) = 2k\int_z^\infty \left(1 + \frac{a^{1/2}}{8\sqrt{\pi(t-z)}}\right)\Omega(t) - \frac{a^{3/2}}{\sqrt{2(t-z)}}\frac{d\Omega(t)}{dt}dt \tag{1}$$

where $\Omega(z)=\Delta f(z)/f_{res}$, k is the cantilever spring constant, a is the oscillation amplitude, z is the tip-sample separation, f

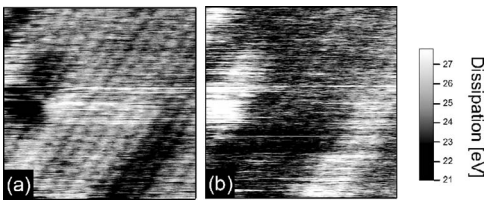

FIG. 9. Molecular-scale ambient FM-AFM simultaneous topography (a) and dissipation (b) images of an EFR thin film on HOPG (30 nm$\times$30 nm, $\Delta f=-52$ Hz, $a=8.9$ nm).

is the resonance frequency of the cantilever, and f_{res} is the unperturbed resonance frequency.[10] This formula is valid for all oscillation amplitudes. The dissipation is calculated from the formula:

$$E = \frac{\pi k a^2}{Q}\left(\frac{A_{exc}}{A_{exc0}} - 1\right) \quad (2)$$

where Q is the quality factor, A_{exc} is the excitation voltage, and A_{exc0} is the excitation voltage away from the surface. Jump-to-contact instabilities do not occur and the retract curve (not shown) follows the approach exactly (i.e., no adhesion from the water layer occurs) and, therefore, we have shown that with this technique we can stably measure the force even in ambient conditions.

Figure 8(a) shows a 500 nm scan with the same cantilever with the corresponding quantified dissipation image [Fig. 8(b)] in units of eV per oscillation. The dissipated energy is greater on the rotaxane monolayer. The contrast in this large-scale image is essentially the same as in the height trace, the sub-molecular motion of the film providing more dissipation channels than the graphite. The molecular-scale dissipation contrast, however, [Fig. 9(b)], captured using the same tip is, by contrast, inverted with respect to the height trace [Fig. 9(a)]. In this image the presence of a defect in the film indicates that the image shows true structure. For the higher resolution image a smaller amplitude, but also a greater frequency shift set point (−52 Hz) is used. The optimum force is probably similar in both cases. Unstable imaging conditions occur if this force is exceeded, presumably because the tip enters the repulsive force region where the feedback polarity is reversed. The inversion of the dissipation image at the molecular scale compared to the meso-scale supports our proposed mechanism of increased dissipation when the number of energy transfer pathways is increased (by increased internal molecular motion), as opposed to a simple tip artefact. If this contrast difference were, for example, due to contact potential differences between graphite and the molecules, then this would imply that at a molecular scale the contrast would not be inverted as in Figs. 6 and 9, but would show similar contrast to topography—i.e., higher above the molecules and lower above the molecular spaces. Observation of increased molecular motion (and hence increased dissipation) as a result of externally induced molecular switching would seem possible, therefore, by dissipation imaging.

Observing switching of material properties of organic films is a specific potential usefulness of the FM-AFM technique in ambient conditions, especially if this is performed at the molecular level.

IV. CONCLUSIONS

We have demonstrated the stable imaging capabilities of the constant amplitude FM-AFM outside of UHV and the high resolution imaging of a soft organic film despite low Q-factor and the native water layer. Accurate determination of the interaction force was also achieved. The energy dissipation was quantitatively measured even at the molecular level, by which means induced sub-molecular motion may be observed in the future. These experiments help to demonstrate the increasing accessibility FM-AFM technique outside of UHV and the potential usefulness of the technique for the development of practical chemical and biological applications, which should help make this important technique more attractive to a wider audience.

ACKLOWLEDGMENT

This research was supported by Science Foundation Ireland Research Grant No. 01/PI.2/C033.

*Author to whom correspondence should be addressed. Email address: farrelaa@tcd.ie

†Email address: David.Leigh@ed.ac.uk

[1] F. J. Giessibl, Science **267**, 68 (1995).

[2] S. Kitamura and M. Iwatsuki, Jpn. J. Appl. Phys., Part 2 **34**, L145 (1995).

[3] M. Bammerlin and R. Luthi, Probe Microsc. **1**, 3 (1997).

[4] K. Kobayashi, H. Yamada, T. Horiuchi, and K. Matsushige, Appl. Surf. Sci. **140**, 281 (1999).

[5] T. Uchihashi, T. Ishida, M. Komiyama, M. Ashino, Y. Sugawara, W. Mizutani, K. Yokoyama, S. Morita, H. Tokumoto, and M. Ishikawa, Appl. Surf. Sci. **157**, 244 (2000).

[6] H. Onishi, A. Sasahara, H. Uetsuka, and T. Ishibashi, Appl. Surf. Sci. **188**, 257 (2002).

[7] T. Fukuma, K. Kobayashi, H. Yamada, and K. Matsushige, J. Appl. Phys. **95**, 4742 (2004).

[8] T. R. Albrecht, P. Grutter, D. Horne, and D. Rugar, J. Appl. Phys. **69**, 668 (1991).

[9] U. Durig, Appl. Phys. Lett. **75**, 433 (1999).

[10] J. E. Sader and S. P. Jarvis, Appl. Phys. Lett. **84**, 1801 (2004).

[11] J. E. Sader, T. Uchihashi, M. J. Higgins, A. Farrell, Y. Nakayama, and S. P. Jarvis, Nanotechnology **16**, S94 (2005).

[12] C. Loppacher, R. Bennewitz, O. Pfeiffer, M. Guggisberg, M. Bammerlin, S. Schär, V. Barwich, A. Baratoff, and E. Meyer, Phys. Rev. B **62**, 13674 (2000).

[13] T. Fukuma, K. Umeda, K. Kobayashi, H. Yamada, and K. Matsushige, Jpn. J. Appl. Phys., Part 1 **41**, 4903 (2002).

[14] C. Loppacher, M. Guggisberg, O. Pfeiffer, E. Meyer, M. Bammerlin, R. Lüthi, R. Schlittler, J. K. Gimzewski, H. Tang, and C. Joachim, Phys. Rev. Lett. **90**, 066107 (2003).

[15] S. P. Jarvis, T. Uchihashi, T. Ishida, H. Tokumoto, and Y. Nakayama, J. Phys. Chem. B **104**, 6091 (2000).

[16] R. Nishi, I. Houda, K. Kitano, Y. Sugawara, and S. Morita, Appl. Phys. A: Mater. Sci. Process. **72**, S93 (2001).

[17] M. Kageshima, H. Jensenius, M. Dienwiebel, Y. Nakayama, H. Tokumoto, S. P. Jarvis, and T. H. Oosterkamp, Appl. Phys. Lett. **188**, 440 (2002).

[18] H. Sekiguchi, T. Okajima, H. Arakawa, S. Maeda, A. Takashima, and A. Ikai, Appl. Surf. Sci. **210**, 61 (2003).

[19] T. Okajima and H. Tokumoto, Jpn. J. Appl. Phys., Part 1 **43**, 4634

(2004).
[20] K. Kobayashi, H. Yamada, and K. Matsushige, Appl. Surf. Sci. **188**, 430 (2002).
[21] A. Sasahara, S. Kitamura, H. Uetsuka, and H. Onishi, J. Phys. Chem. B **108**, 15735 (2004).
[22] T. Fukuma, T. Ichi, K. Kobayashi, H. Yamada, and K. Matsushige, Appl. Phys. Lett. **86**, 134103 (2005).
[23] H. Hölscher, B. Gotsmann, and A. Schirmeisen, Phys. Rev. B **68**, 153401 (2003).
[24] H. Hölscher and B. Anczykowski, Surf. Sci. **579**, 201 (2005).
[25] D. Anselmetti, M. Dreier, R. Lüthi, T. Richmond, E. Meyer, J. Frommer, and H.-J. Güntherodt, J. Vac. Sci. Technol. B **12**, 1500 (1994).
[26] *Molecular Catenanes, Rotaxanes and Knots*, edited by J.-P. Sauvage and C. Dietrich-Buchecker (Wiley-VCH, Weinheim, 1999).
[27] V. Balzani, A. Credi, F. M. Raymo, and J. F. Stoddart, Angew. Chem., Int. Ed. **39**, 3348 (2000).
[28] Special Issue on Molecular Machines: Acc. Chem. Res. **34**, 409 (2001).
[29] M. Venturi, A. Credi, and V. Balzani, *Molecular Devices and Machines-A Journey into the Nanoworld* (Wiley-VCH, Weinheim, 2003).
[30] F. G. Gatti, D. A. Leigh, S. A. Nepogodiev, A. M. Z. Slawin, S. J. Teat, and J. K. Y. Wong, J. Am. Chem. Soc. **123**, 5983 (2001).
[31] F. G. Gatti, S. Leòn, J. K. Y. Wong, G. Bottari, A. Altieri, M. A. Farran Morales, S. J. Teat, C. Frochot, D. A. Leigh, A. M. Brouwer, and F. Zerbetto, Proc. Natl. Acad. Sci. U.S.A. **100**, 10 (2003).
[32] A. Altieri, G. Bottari, F. Dehez, D. A. Leigh, J. K. Y. Wong, and F. Zerbetto, Angew. Chem., Int. Ed. **42**, 2296 (2003).
[33] A. Altieri, F. G. Gatti, E. R. Kay, D. A. Leigh, F. Paolucci, A. M. Z. Slawin, and J. K. Y. Wong, J. Am. Chem. Soc. **125**, 8644 (2003).
[34] D. A. Leigh and E. M. Pérez, Chem. Commun. (Cambridge) **2004**, 2262.
[35] F. Biscarini, M. Cavallini, D. A. Leigh, S. León, S. J. Teat, J. K. Y. Wong, and F. Zerbetto, J. Am. Chem. Soc. **124**, 225 (2002).
[36] T. Gase, D. Grando, P.-A. Chollet, F. Kajzar, A. Murphy, and D. A. Leigh, Adv. Mater. (Weinheim, Ger.) **11**, 1303 (1999).
[37] I. Willner, V. Pardo-Yissar, E. Katz, and K. T. Ranjit, J. Electroanal. Chem. **497**, 172 (2001).
[38] S. Chia, J. Cao, J. F. Stoddart, and J. I. Zink, Angew. Chem., Int. Ed. **40**, 2447 (2001).
[39] M. Cavallini, R. Lazzaroni, R. Zamboni, F. Biscarini, D. Timpel, F. Zerbetto, G. J. Clarkson, and D. A. Leigh, J. Phys. Chem. B **105**, 10826 (2001).
[40] B. Long, K. Nikitin, and D. Fitzmaurice, J. Am. Chem. Soc. **125**, 5152 (2003).
[41] B. Long, K. Nikitin, and D. Fitzmaurice, J. Am. Chem. Soc. **125**, 15490 (2003).
[42] H.-R. Tseng, D. Wu, N. X. Fang, X. Zhang, and J. F. Stoddart, Bandaoti Xuebao **5**, 111 (2004).
[43] T. Jun Huang, H.-R. Tseng, L. Sha, W. Lu, B. Brough, A. H. Flood, B.-D. Yu, P. C. Celestre, J. P. Chang, J. F. Stoddart, and C.-M. Ho, Nano Lett. **4**, 2065 (2004).
[44] E. Katz, L. Sheeney-Haj-Ichia, and I. Willner, Angew. Chem., Int. Ed. **43**, 3292 (2004).
[45] E. Katz, O. Lioubashevsky, and I. Willner, J. Am. Chem. Soc. **126**, 15520 (2004).
[46] K. Kobayashi, H. Yamada, K. Umeda, T. Horiuchi, S. Watanabe, T. Fujii, S. Hotta, and K. Matsushige, Appl. Phys. A: Mater. Sci. Process. **72**, S97 (2001).
[47] H. Yamada, T. Fukuma, K. Umeda, K. Kobayashi, and K. Matsushige, Appl. Surf. Sci. **188**, 391 (2002).
[48] K. Tamada, H. Akiyama, T.-X. Wei, and S.-A. Kim, Langmuir **19**, 2306 (2003).
[49] Z. Wang, M. J. Cook, A.-M. Nygård, and D. A. Russell, Langmuir **19**, 3779 (2003).
[50] Z. Wang, A.-M. Nygård, M. J. Cook, and D. A. Russell, Langmuir **20**, 5850 (2004).
[51] T. Hugel, N. B. Holland, A. Cattani, L. Moroder, M. Seitz, and H. E. Gaub, Science **296**, 1103 (2002).
[52] K. Kobayashi, H. Yamada, H. Itoh, T. Horiuchi, and K. Matsushige, Rev. Sci. Instrum. **72**, 4383 (2001).
[53] S. P. Jarvis, T. Ishida, T. Uchihashi, Y. Nakayama, and H. Tokumoto, Appl. Phys. A: Mater. Sci. Process. **72**, S129 (2001).
[54] B. Gotsmann, C. Seidel, B. Anczykowski, and H. Fuchs, Phys. Rev. B **60**, 11051 (1999).
[55] T. Ichii, T. Fukuma, K. Kobayashi, H. Yamada, and K. Matsushige, Appl. Surf. Sci. **210**, 99 (2003).
[56] T. Fukuma, T. Ichi, K. Kobayashi, H. Yamada, and K. Matsushige, J. Appl. Phys. **95**, 1222 (2004).
[57] R. García and R. Pérez, Surf. Sci. Rep. **47**, 197 (2002).
[58] M. A. Lantz, H. J. Hug, R. Horrmann, P. J. A. van Schendel, P. Kappenberger, S. Martin, A. Baratoff, and H.-J. Guntherodt, Science **291**, 2580 (2001).
[59] T. Uchihashi, M. J. Higgins, S. Yasuda, S. P. Jarvis, S. Akita, Y. Nakayama, and J. E. Sader, Appl. Phys. Lett. **85**, 3575 (2004).